Article:
Enema, J.O., Umoh, U.F., Johnson, E.C. et al. (2 more authors) (2025) Isolation and characterisation of Docosanoic acid, Quercetin and Vitexin from Dennettia tripetala Bak. f. Root and stem bark and their in-vivo anti-inflammatory and analgesic activities. Journal of Advances in Medicine and Medical Research, 37 (3). pp. 209-228. ISSN 2456-8899

https://doi.org/10.9734/jammr/2025/v37i35758

Journal of Advances in Medicine and Medical Research

Volume 37, Issue 3, Page 209-228, 2025; Article no.JAMMR.132064
ISSN: 2456-8899, NLM ID: 101711724
(Past name: British Journal of Medicine and Medical Research, Past ISSN: 2231-0614, NLM ID: 101570965)

Isolation and Characterisation of Docosanoic Acid, Quercetin and Vitexin from *Dennettia tripetala* Bak. f. Root and Stem Bark and their *In-vivo* Anti-inflammatory and Analgesic Activities

Enema, Onojah John [a*], Umoh, Uwemedimo Francis [a], Ekarika, C. Johnson [b], Khalid, Doudin [c] and Johnny, I. Imoh [a]

[a] Department of Pharmacognosy and Natural Medicine, Faculty of Pharmacy, University of Uyo, Uyo, Nigeria.
[b] Department of Pharmaceutical and Medicinal Chemistry, Faculty of Pharmacy, University of Uyo, Uyo, Nigeria.
[c] Department of Mathematical and Physical Sciences, The University of Sheffield, Sheffield, S3 7HF, United Kingdom.

Authors' contributions

This work was carried out in collaboration among all authors. All authors read and approved the final manuscript.

Article Information

DOI: https://doi.org/10.9734/jammr/2025/v37i35758

Open Peer Review History:
This journal follows the Advanced Open Peer Review policy. Identity of the Reviewers, Editor(s) and additional Reviewers, peer review comments, different versions of the manuscript, comments of the editors, etc are available here: https://pr.sdiarticle5.com/review-history/132064

Original Research Article

Received: 24/12/2024
Accepted: 26/02/2025
Published: 28/02/2025

**Corresponding author: E-mail: pgsjeonojah@uniuyo.edu.ng, enemaoj@gmail.com;*

Cite as: *John , Enema, Onojah, Umoh, Uwemedimo Francis, Umoh, Uwemedimo Francis, Ekarika, C. Johnson, Khalid, Doudin, and Johnny, I. Imoh. 2025. "Isolation and Characterisation of Docosanoic Acid, Quercetin and Vitexin from Dennettia Tripetala Bak. F. Root and Stem Bark and Their In-Vivo Anti-Inflammatory and Analgesic Activities". Journal of Advances in Medicine and Medical Research 37 (3):209-28. https://doi.org/10.9734/jammr/2025/v37i35758.*

ABSTRACT

Dennettia tripetala Baker f. (Annonaceae) is widely used in African traditional medicine for managing diabetes, inflammation, pain, and other ailments due to its diverse phytochemical composition. This study aimed to isolate and characterize bioactive compounds from the root and stem bark of *D. tripetala* and evaluate their anti-inflammatory and analgesic properties through *in vivo* models. The plant materials were extracted using 70% aqueous methanol, and the extracts were partitioned into n-hexane, dichloromethane, ethyl acetate, and n-butanol fractions. Compounds were isolated through open-column chromatography and thin layer chromatography and characterized using ^{1}H NMR, ^{13}C NMR, and FTIR spectroscopy. Ethical approval was obtained from the University of Uyo Health Research Ethics Committee for animal studies. Anti-inflammatory activity was evaluated using egg albumin and xylene-induced oedema models, while analgesic activity was assessed using formalin-induced paw licking and hot plate tests, respectively. Data were analyzed using one-way ANOVA, with significance level set at $p<0.05$. The dichloromethane and ethyl acetate fractions exhibited the highest anti-inflammatory activity, with the root extract at 447 mg/kg significantly inhibiting egg albumin-induced oedema by 81% at 5 hours, compared to 77% for aspirin. In the xylene-induced oedema model, the root extract at 670 mg/kg achieved 76% inhibition, comparable to the standard drug. Analgesic effects were most pronounced in the formalin test, where the root extract reduced paw licking duration by 85% in the late phase. Isolated compounds, including quercetin, vitexin, and docosanoic - nonacosyl ester acid were carried out using spectroscopic methods. These findings validate the traditional use of *D. tripetala* and highlight its potential as a source of natural therapeutic agents.

Keywords: Dennettia tripetala; anti-inflammatory; analgesic; phytochemical properties; isolation and characterization.

1. INTRODUCTION

All over the world, there is a growing demand for medicinal plants. Beyond treating diseases, people are increasingly turning to these plants as natural alternatives to synthetic drugs, which may pose health risks due to their numerous side effects. Most plants are used in our everyday cooking as herbs, spices, seasonings, teas, enemas, and preservatives and sometimes as insecticides. Studies have been carried out to verify the efficacy of some medicinal plants in the prevention and treatment of diseases (Soforowa et al., 2013; Adesina and Johnny, 2021).

Dennettia tripetala is utilized in traditional medicine in Africa for the treatment of various ailments including inflammation and pains, diabetes and cancer. This broad bioactivity has been reported to be due to the diverse group of phytoconstituents in the plant including annonaceous acetogenins, as well as huge deposits of flavonoids and alkaloids (Enema, et al., 2024).

Reports have shown that there is an increasing trend of chronic diseases like cancer, inflammations and pains and growing resistance to conventional pharmaceuticals like nonsteroidal anti-inflammatory drugs (NSAIDs) and opioids as well as the side effects often associated with conventional treatments, this emphasizes the urgent need for novel therapeutic agents derived from natural sources (Eseyin et al., 2017; Tsai et al., 2019; Pahwa et al., 2021).

This study focused on isolating and identifying bioactive compounds from the root and stem bark of *D. tripetala* and assessing the anti-inflammatory and pain-relieving effects of the various extracts and fractions using *in vivo* models.

2. MATERIALS AND METHODS

2.1 Plant Collection and Identification

The stem bark and root of *D. tripetala* were collected from Itak Ikot Akap village in Ikono Local Government Area, Akwa Ibom State, Nigeria. The plant was identified by Dr. Imeh Imoh Johnny of the Department of Pharmacognosy and Natural Medicine, Faculty of Pharmacy, University of Uyo, Uyo and authenticated by Prof. Mrs. M.E Bassey of the Department of Botany and Ecological Studies, Faculty of Biological Sciences, University of Uyo, Uyo and a voucher specimen deposited in the herbarium. The voucher number UUPH A2(i) was assigned.

2.2 Extraction and Partitioning

The stem bark and root of *D. tripetala* were air-dried and coarsely powdered with a hammer mill. About 3 kg of each of the powdered plant materials were extracted in 70% aqueous methanol. The extract was dried, weighed, and stored in a refrigerator. The dried extracts were then partitioned using various solvents including n-hexane, dichloromethane, ethyl acetate, and n-butanol, aqueous, respectively to obtain the respective fractions after drying.

2.3 Acute Toxicity Testing (LD_{50})

An Acute toxicity study was done using the method of Lorke (1983) with slight modifications. Mice were randomized and divided into groups of three mice per group. The animals were starved of food 24 hours before the experiment. The aqueous methanol extract was administered intraperitoneally (IP) in a dose range of 100-3000 mg/kg body weights.

2.4 Egg Albumin-Induced Oedema

In this model, albino mice of either sex were randomized and divided into five groups of five animals each. Group one animals were pretreated with distilled water (10 mL/kg), groups 2 to 4 were pretreated with 224 mg/kg, 447 mg/kg and 670 mg/kg for the root and 324 mg/kg, 648 mg/kg and 972 mg/kg for the stem bark extract, respectively, thirty (30) minutes before the induction of edema with fresh egg albumin while group five animals received the standard drug acetylsalicylic acid (ASA 100 mg/kg). The linear circumference of the injected paws was assessed with vernier calipers before and at thirty-minute intervals for 5 hours following the administration of egg albumin (Okokon et al*.,* 2008).

2.5 Formalin-Induced Paw Licking in Mice

The procedure followed was similar to that previously described by Hunskaar and Hole (1987) and Nwafor and Okwuasaba (2003). Twenty microliters (20 µL) of 2.5% formalin solution (0.9% formaldehyde) was made up in phosphate buffer solution (PBS concentration: NaCl, 137 mM; KCl, 2.7 mM and phosphate buffer, 10 mM) and injected into the undersurface of the right hind paw subcutaneously. The time that the animals spent licking the injected paw was taken as a measure of pain with the first phase of response at 5 minutes and second phase (15-30 minutes) after formalin injection. Thirty minutes before the challenge with buffered formalin, albino mice were randomly divided into five groups of 5 animals in each group. Animals in group 1 were pretreated with distilled water (10 ml/kg), groups 2-4 extract (224 - 972 mg/kg, IP), and group 5 ASA (100 mg/k, IP). The fractions were also evaluated at a dose of 447 - 648 mg/kg with sodium carbonate as control.

2.6 Thermally-Induced Pain in Mice

The effect of the extract on the hot plate was investigated in adult mice. The procedure was basically similar to the one earlier described by Vaz et al. (1996). Adult mice were put into a glass beaker of 50cm diameter and placed on a hot plate that was kept at 45 ± 1°C. The time(s) between being placed on the hot plate and licking the paws were recorded. Animals were grouped as described above and pretreated the same 30 minutes prior to being placed on the hot plate.

2.7 Xylene-Induced Ear Oedema

Male and female albino mice were randomly divided into six groups of six animals in each group. Two (2) drops of xylene topically applied to the inner surface portion of the right ear and allowed for 15 minutes was used to induce Inflammation (Mbagwu et al., 2007). Group 1 received distilled water (10 ml/kg; ip), animals in groups 2-4 were made to receive 30-90 mg/kg of extract intraperitoneally, group 5 animals received dexamethasone and group 6 received extract plus dexamethasone (4 mg/kg, ip) 30 minutes before induction of inflammation. The animals were sacrificed using chloroform anesthesia and their left and right ears cut off. The difference in weights indicated the degree of xylene-induced oedema (Tjolsen et al., 1992). The fractions were assessed at a dose of 447 - 648 mg/kg with sodium carbonate as control.

2.8 Isolation of AZ

About 26 g of the dichloromethane extract from the root was subjected to open-column chromatography. Silica gel (60–200 mesh) was used as the stationary phase, while a solvent gradient starting from 100% n-hexane to mixtures with dichloromethane, ethyl acetate, and methanol was used as the mobile phase. This resulted in the collection of 116 fractions from the first column. Each fraction was analyzed using Thin Layer Chromatography (TLC) with

solvent systems such as n-hexane and dichloromethane in ratios of 1:9, 3:7, 2:8, and 50:50. Fractions with similar TLC profiles was bulked into 44Q (2724 mg), A30 (1968 mg), 84D (478 mg), and 93B (1102 mg).

Further purification of A30 (1968 mg) was conducted using open-column chromatography with a similar gradient of n-hexane, dichloromethane, and ethyl acetate. TLC analysis of subfractions resulted in bulking into A1(320 mg), A2 (546 mg), A3 (418 mg), A4 (288 mg), and A5 (244 mg), respectively due to similar TLC profiles. Sample A2 (546 mg) was further subjected to open-column chromatography. The fractions were bulked into A2X (164 mg), A2Y (163 mg), A2Q (87 mg), and A2M (52 mg), respectively. Sample A2Y (163 mg) was further purified using preparative TLC. Two bands were scraped and labelled as A100 (69 mg) and AZ (9 mg). The fractions were analyzed using TLC with various solvent systems, namely: different ratios of n-hexane and dichloromethane (1:9, 3:7, 2:8, 50:50), 100% dichloromethane, and dichloromethane with ethyl acetate (9:1 and 7:2). A single spot consistently appeared on the TLC plate, confirming purity. AZ was weighed, and its final weight was recorded as 9 mg.

2.9 Isolation of B40

Bulked fraction 93B (1102 mg), obtained from the initial 116 fractions was further subjected to purification through open-column chromatography. The elution began with 100% n-hexane and progressed to dichloromethane, ethyl acetate, and methanol in varying proportions. TLC analysis of the collected subfractions indicated the presence of distinct groups, which were bulked into AQ (310 mg), B1(286 mg), and B20 (372 mg), respectively based on their chemical profiles. The B1 (286 mg) fraction was then subjected to preparative TLC using 100% dichloromethane as the solvent system. The dried sample was dissolved, spotted on preparative TLC plates, and developed in a TLC tank. Two bands were scraped; B40 (17 mg) and B12 (174 mg), respectively. Consistent TLC results under various solvent systems (e.g., n-hexane and dichloromethane in ratios 1:9, 3:7, 2:8, and 50:50) confirmed the purity of B40. The weight of the compound was recorded as 17 mg.

2.10 Isolation of OX2

Sample B20 (322 mg) another subfraction of 93B was further purified using preparative TLC with 100% dichloromethane as the solvent system. The dried B20 sample was dissolved, applied to the preparative TLC plate, and developed in the TLC tank. After visualization under UV light, three distinct bands were identified and scraped into separate beakers: OX2 (15 mg), O1 (208 mg), and O2 (66 mg), respectively. Different solvent systems including n-hexane and dichloromethane in ratios like 1:9, 3:7, 2:8, and 50:50, as well as dichloromethane and ethyl acetate in ratios such as 9:1 and 7:2 were used in analyzing fraction OX2. This analysis confirmed the presence of a single spot, indicating purity. OX2 was then weighed, with a final weight of 15 mg.

3. RESULTS AND DISCUSSION

3.1 Yield of Extract and Fractions

The total yield of extracts was 102 g for the stem bark methanol extract and 138 g for the root extract of *D. tripetala.* The yield of fractions and percentage yield are presented in Table 1. The dichloromethane fraction of the stem bark had the most yield and was closely followed by the aqueous fraction of the root extract. The n-hexane fraction of the root and stem bark extracts had the least yield when compared with other fractions, respectively.

3.2 Egg Albumin Anti-inflammatory Study of EPFR and EPFS

The results of the egg albumin anti-inflammatory effects are displayed in Table 2. The result showed that the root extract at 447 mg/kg (the median) dose had more activity when compared to other doses tested. This was closely followed

Table 1. Yield of Fractions

Fractions	Root (g)	Percentage Yield (%)	Stem bark (g)	Percentage Yield (%)
n-hexane	13.2	10.0	9.7	10.0
Dichloromethane	26.2	19.0	22.5	22.0
Ethyl acetate	18.0	13.0	14.0	14.0
n-butanol	13.4	10.0	17.3	17.0
Aqueous	28.1	20.0	19.8	19.0

by the high dose of the root extract at 670 mg/kg. The result showed that the inhibition of egg albumin-induced oedema was not dose-dependent.

3.3 Formalin Induced Paw Edema of EPFS and EPFR

Table 3 shows the result of the formalin-induced paw oedema in mice. Like that of the egg albumin-induced oedema in mice, the result also showed that the median dose of the root extract of *D. tripetala* had the most activity at most time intervals followed by the high dose at 670 mg/kg.

3.4 Hot Plate Analgesia Comparison of EPFS and EPFR

The hot plate analgesia result is also displayed in Table 4. The result showed that the median dose was the most active dose followed by the high dose at 670 mg/kg. When compared to the stem bark extract, the root had more activity. This result also shows that the activity is not dose-dependent which may be attributed to the pharmacokinetics properties of the extracts.

3.5 Hot Plate Analgesia Comparison of Fractions of EPFR

The result of the hot plate analgesia comparisons of the fractions in Table 5 also showed that the DCM fraction had the most activity and was closely followed by the ethyl acetate fraction and with the n-butanol fraction low dose showing the least activity.

3.6 Xylene-induced Edema Inhibition of EPFS and EPFR

Table 6 shows that the xylene-induced oedema inhibition also showed that the root extract was more active at various doses than the stem bark extract.

3.7 Xylene-induced Anti-inflammatory Inhibition of Fractions EPFR

The fractions of the stem bark and root bark extract were also compared in Table 7. The result revealed that the dichloromethane fraction had the most activity followed by the ETH fraction.

3.8 ^{1}H NMR Analysis of Sample AZ

Table 8 and Fig. 1, reveal the ^{1}H NMR spectrum peaks of sample AZ corresponding to CH_2 groups near oxygen (3.98 ppm) and carbonyl (2.22 ppm) groups, along with signals for a long alkyl chain (1.54, 1.18 ppm) and terminal methyl groups (0.81 ppm), suggesting the presence of ester linkages and a fatty acid-like structure.

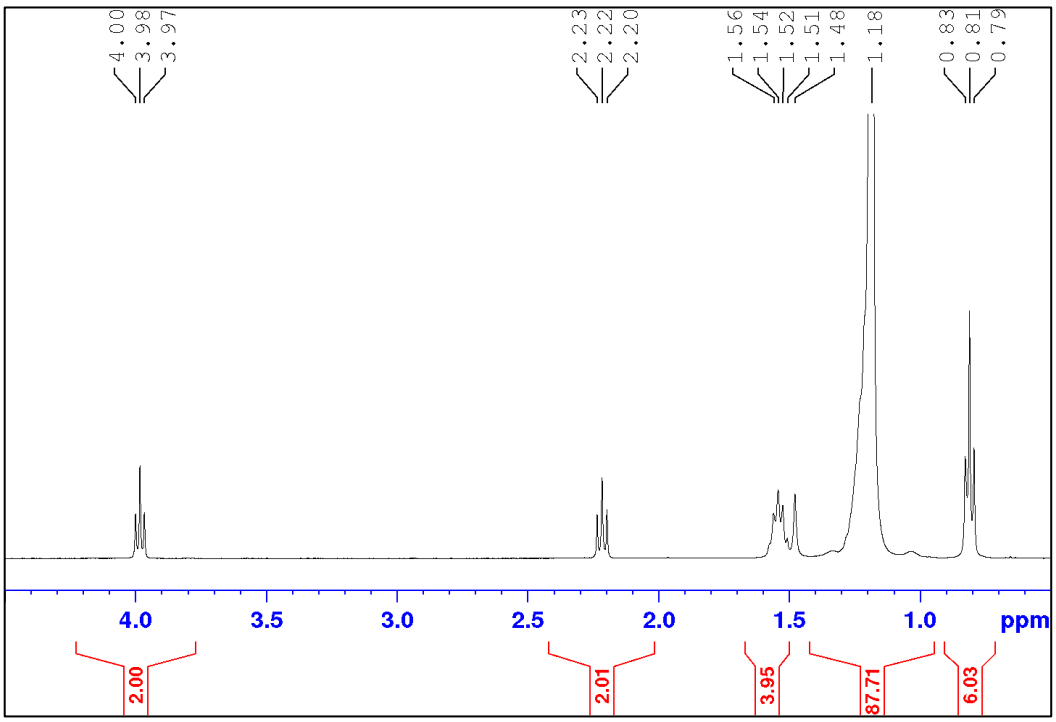

Fig. 1. ^{1}H NMR spectra of AZ

Table 2. Egg albumin anti-inflammatory analysis of EPFR and EPFS

	Mean oedema volume (ml) at different hours						
Treatment (mg/kg)	**0h**	**0.5h**	**1h**	**2h**	**3h**	**4h**	**5h**
N. Saline 10	2.236 ± 0.110^{ns}	1.596 ± 0.058*	1.138 ± 0.076^{ns}	0.990 ± 0.055^{ns}	0.854 ± 0.028^{ns}	0.756 ± 0.036^{ns}	0.674 ± 0.013^{ns}
ASA 100	2.12 ± 0.072^{ns}	1.172 ± 0.045*	0.786 ± 0.044*	0.506 ± 0.051*	0.438 ± 0.041*	0.292 ± 0.023*	0.172 ± 0.048*
EPFR 224	2.152 ± 0.082^{ns}	1.048 ± 0.089*	0.932 ± 0.051^{ns}	0.814 ± 0.041^{ns}	0.704 ± 0.015*	0.32 ± 0.050*	0.198 ± 0.047*
EPFR 447	2.274 ± 0.010^{ns}	0.876 ± 0.102*	0.588 ± 0.011*	0.436 ± 0.095*	0.32 ± 0.032*	0.21 ± 0.019*	0.126 ± 0.037*
EPFR 670	2.146 ± 0.051^{ns}	1.012 ± 0.071*	0.704 ± 0.096*	0.474 ± 0.059*	0.314 ± 0.037*	0.228 ± 0.039*	0.138 ± 0.026*
EPFS 324	2.266 ± 0.044^{ns}	1.228 ± 0.010*	0.712 ± 0.039*	0.552 ± 0.037*	0.428 ± 0.031*	0.308 ± 0.049*	0.186 ± 0.043*
EPFS 648	2.152 ± 0.036^{ns}	1.092 ± 0.047*	0.816 ± 0.044*	0.572 ± 0.039*	0.434 ± 0.041*	0.336 ± 0.018*	0.248 ± 0.034*
EPFS 972	2.296 ± 0.066^{ns}	1.102 ± 0. 041*	0.882 ± 0.038^{ns}	0.708 ± 0.028*	0.576 ± 0.038*	0.392 ± 0.030*	0.256 ± 0.213*

Where;
ASA - Aspirin
EPFR - D. tripetala root extract
EPFS - D. tripetala stem bark extract

Table 3. Effects of EPFS and EPFR on formalin induced paw oedema

	Time (min)					
Treatment (mg/kg)	**5 min**	**10 min**	**15 min**	**20 min**	**25 min**	**30 min**
Saline 10	22.2 ± 1.281^{ns}	13.2 ± 1.594^{ns}	8.2 ± 0.583^{ns}	7.2 ± 1.594^{ns}	5.2 ± 1.393^{ns}	5.2 ± 0.663^{ns}
ASA 100	11.6 ± 0.748*	6.6 ± 1.166^{ns}	3.8 ± 0.583*	2.2 ± 0.8^{ns}	1.8 ± 0.489^{ns}	1.2 ± 0.583*
EPFS 324	12.2 ± 3.087*	12.6 ± 0.812^{ns}	6.4 ± 0.872^{ns}	4 ± 0.834^{ns}	4.6 ± 0.937^{ns}	2.8 ± 0.860^{ns}
EPFS 648	15.0 ± 1.949*	12.2 ± 0.374^{ns}	4.2 ± 1.356^{ns}	4.6 ± 1.029^{ns}	2.6 ± 0.678^{ns}	2.6 ± 0.812^{ns}
EPFS 972	14.0 ± 1.581*	4.2 ± 0.734*	4.4 ± 2.227*	2.2 ± 0.663^{ns}	2.4 ± 0.871^{ns}	1.2 ± 0.583*
EPFR 224	12.0 ± 1.581*	5.0 ± 1.761*	3.0 ± 0.547*	2.0 ± 0.837^{ns}	2 ± 0.774^{ns}	1.4 ± 0.748*
EPFR 447	10.4 ± 0.60*	4.0 ± 0.775*	2.0 ± 0.447*	0.6 ± 0.40*	0.6 ± 0.244^{ns}	0.8 ± 0.489*
EPFR 671	8.2 ± 0.860*	1.8 ± 0.969*	2.2 ± 0.8*	1.0 ± 0.548*	0.2 ± 0.2^{ns}	0.6 ± 0.245*

Table 4. Hot plate analgesia comparison of extracts (EPFS and EPFR)

Treatment (mg/kg)	Time (s)
Saline 10	13.17 ± 2.522*
ASA 100	29.00 ± 0.365*
EPFS 324	23.83 ± 1.046*
EPFS 648	25.33 ± 1.406*
EPFS 972	26.5 ± 1.176*
EPFR 224	27.67 ± 0.615*
EPFR 447	29.33 ± 0.333*
EPFR 670	29.00 ± 0.516*

Table 5. Hot plate analgesia comparison of fractions of EPFR

Treatment (mg/kg)	Time (s)
Saline (10	13.17 ± 2.522*
ASA (100	29.00 ± 0.365*
EPFR NH 224	25.17 ± 0.601*
EPFR NH 447	26.17 ± 0.601*
EPFR NH 671	27.50 ± 0.428*
EPFR DCM 224	28.67 ± 0.333*
EPFR DC M 447	29.00 ± 0.365*
EPFR DCM 671	29.83 ± 0.167*
EPFR ETH 224	27.83 ± 0.543*
EPFR ETH 447	27.67 ± 0.667*
EPFR ETH 671	28.00 ± 0.447*
EPFR nBT 224	22.00 ± 0.183*
EPFR nBT 447	24.00 ± 1.183*
EPFR nBT 671	24.67 ± 1.256*
EPFR AQ 224	25.50 ± 0.671*
EPFR AQ 447	24.83 ± 1.327*
EPFR AQ 671	25.33 ± 1.330*

Table 6. Xylene anti-inflammatory edema inhibition of EPFS and EPFR

Xylene anti-inflammatory oedema inhibition		
Treatment (mg/kg)	**% oedema degree**	**% oedema inhibition**
ASA 100	8.89 ± 1.4396*	77
EPFS 324	16.3 ± 3.413*	58
EPFS 648	11.88 ± 2.457*	69
EPFS 972	10.25 ± 1.892*	73
EPFR 224	12.81 ± 3.355*	67
EPFR 447	9.928 ± 1.733*	74
EPFR 670	9.144 ± 1.807*	76

Table 7. Xylene anti-inflammatory oedema inhibition of fractions EPFR

Xylene anti-inflammatory oedema inhibition		
Treatment (mg/kg)	**% oedema degree**	**% oedema inhibition**
ASA 100	8.89 ± 1.483*	77
NH 224	32 ± 4.231ns	18
NH 447	22.12 ± 5.51 ns	43
NH 670	22.25 ± 3.478 ns	43
DCM 224	10.14 ± 1.235*	74
DCM 447	10.53 ± 2.628*	73
DCM 670	14.02 ± 3.021*	64

Xylene anti-inflammatory oedema inhibition		
Treatment (mg/kg)	**% oedema degree**	**% oedema inhibition**
ETH 224	23.51 ± 7.705 ^{ns}	17
ETH 447	16.97 ± 2.302*	56
ETH 670	18.29 ± 5.434*	53
nBT 224	38.22 ± 6.271 ^{ns}	2
nBT 447	34.38 ± 2.421 ^{ns}	12
nBT 670	14.89 ± 2.292*	61
AQ 224	27.2 ± 6.594 ^{ns}	30
AQ 447	18.71 ± 2.945*	51
AQ 670	29.48 ± 5.59 ^{ns}	25

Where;
NH - n-hexane fraction
DCM - dichloromethane fraction
ETH - Ethyl acetate fraction
nBT - n-butanol fraction
AQ - Aqueous fraction

3.9 ^{13}C NMR Analysis of Sample AZ

Fig. 2 and Table 9 show that the ^{13}C NMR spectrum displays a strong carbonyl signal at 174.0 ppm, confirming an ester or carboxyl group, along with peaks for CH_2 groups attached to oxygen (64.4 ppm) and carbonyl (34.4 ppm), and several signals from long alkyl chains (29.7–14.1 ppm), further supporting an esterified long-chain fatty structure.

3.10 FTIR Analysis of Sample AZ

The FTIR spectrum of sample AZ is presented in Fig. 3 and Table 10 showing the functional groups. A sharp C=O stretch at 1736 cm^{-1} (confirming ester carbonyl groups), and a C-O stretch at 1048 cm^{-1}, consistent with ester or ether linkages, pointing to ester functionalities and possible hydroxyl groups in the structure.

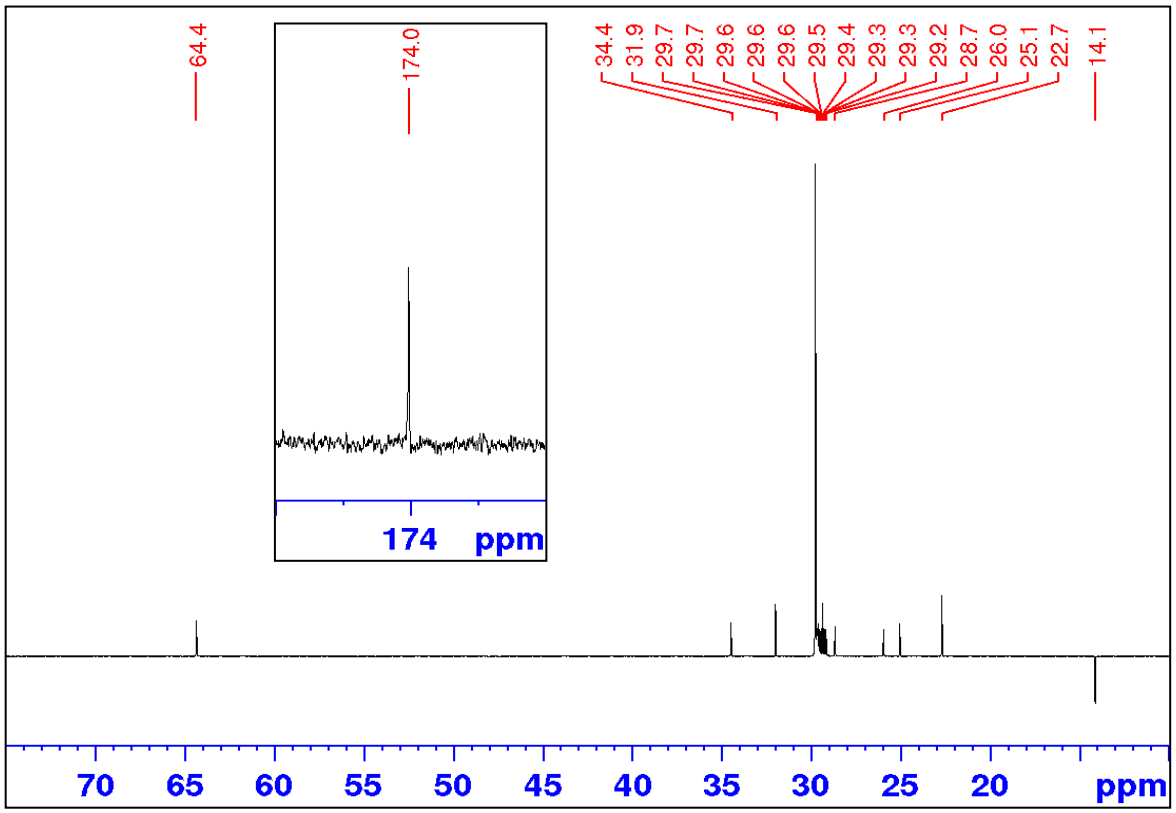

Fig. 2. ^{13}C NMR spectra of AZ

Table 8. ^{1}H NMR spectra information of sample AZ

Peak (δ ppm)	Multiplicity (J, Hz)	Number of Protons (Sample AZ)	Literature Peaks (NCBI, 2024)	Functional Group/Assignment	Significant Peaks for Identification
3.98	t (J = 6.7 Hz)	2H	3.9–4.0 t	-CH_2 next to oxygen (R-CH_2-O)	Yes, indicates CH_2 near oxygen
2.22	t (J = 7.5 Hz)	2H	2.2–2.3 t	-CH_2 next to carbonyl (R-CH_2-C=O)	Yes, indicates CH_2 near carbonyl
1.54	p (J = 6.8 Hz)	5H	1.5–1.6 p	Methylene groups (-CH_2-)	No, general alkyl chain peaks
1.18	m	88H	1.1–1.2 m	Long alkyl chain (-CH_2-)	No, indicates long alkyl chain
0.81	t (J = 6.8 Hz)	6H	0.8–0.9 t	Terminal methyl (-CH_3)	No, typical methyl group signal

Table 9. ^{13}C NMR spectra data for sample AZ

Peak (δ ppm)	Sample AZ	Literature Peaks (NCBI, 2024)	Functional Group/Assignment	Significant Peaks for Identification
174.03	Present	170–175	Carbonyl group (C=O, ester or acid)	Yes, indicates ester/carboxyl group
64.41	Present	60–65	-CH_2 next to oxygen (R-CH_2-O)	Yes, confirms CH_2 near oxygen
34.44	Present	34–35	-CH_2 near carbonyl group	Yes, confirms CH_2 next to C=O
31.94	Present	31–32	Alkyl chain (-CH_2-)	No, part of long alkyl chain
29.71–29.18	Present (multiple peaks)	29–30	Long alkyl chain (-CH_2-)	No, typical alkyl chain signals
28.67	Present	28–29	Alkyl chain (-CH_2-)	No, typical alkyl chain signals
25.96	Present	25–26	Alkyl chain (-CH_2-)	No, typical alkyl chain signals
25.05	Present	24–25	Alkyl chain (-CH_2-)	No, typical alkyl chain signals
22.7	Present	22–23	Terminal methyl (-CH_3)	No, typical methyl group
14.12	Present	14–15	Terminal methyl (-CH_3)	No, typical methyl group

Table 10. FTIR spectra data for sample AZ

Peak (cm^{-1})	Sample AZ	Literature Peaks (NCBI, 2024)	Functional Group/Assignment	Significant Peaks for Identification
1736	Present	1720–1750	C=O stretch (Carbonyl in esters)	Yes, confirms ester carbonyl (C=O) group
1457	Present	1450–1470	CH_2 bending (Alkyl chains)	No, typical CH_2 bending
1048	Present	1050–1150	C-O stretch (Alcohols, ethers, esters)	Yes, confirms C-O bond in esters or ethers

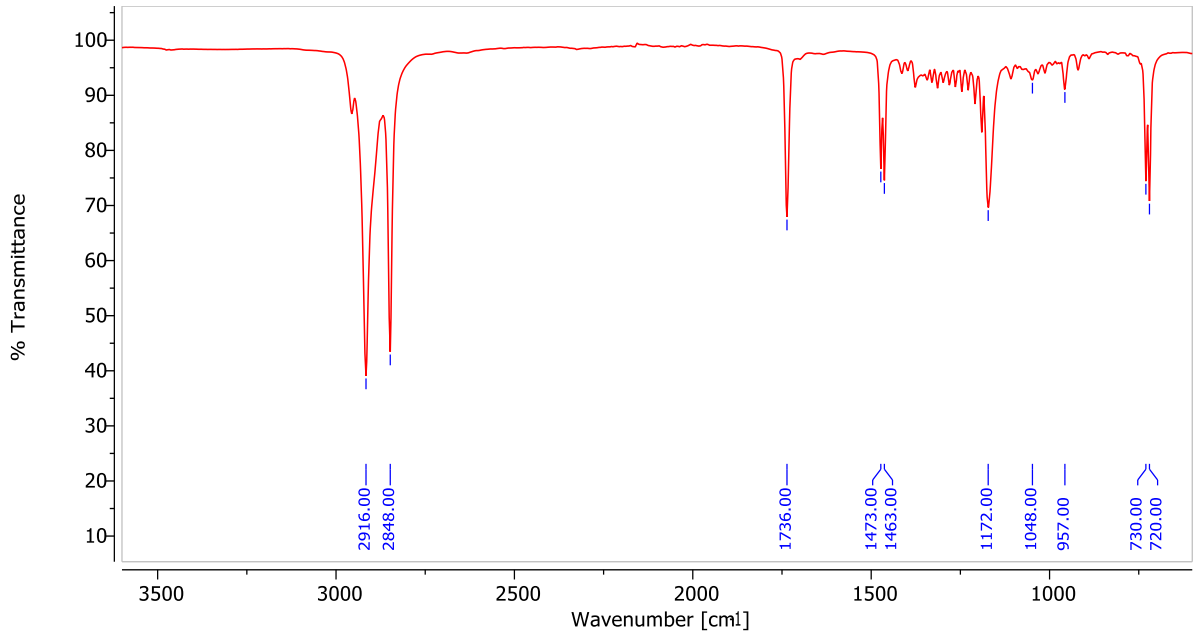

Fig. 3. FTIR spectra of AZ

Combined analysis of ^{1}H NMR, ^{13}C NMR, and FTIR spectra identifies the compound as an ester of a long-chain fatty acid. Characteristic spectral features, including signals for a long alkyl chain and ester carbonyl (C=O) groups, confirm its saturated nature. ^{1}H NMR integrals suggest the presence of approximately 48 methylene ($-CH_2-$) units, two terminal methyl groups, and a carbonyl group, corresponding to a molecular formula of $C_{51}H_{102}O_2$. The data indicate that the compound is likely docosanoic acid ester (nonacosyl ester), known for its applications in cosmetics and pharmaceuticals, as well as its anti-inflammatory and antioxidant properties.

3.11 ^{1}H NMR Analysis of Sample B40

The ^{1}H NMR spectrum of sample B40 shows signals for several hydroxyl (O-H) groups between δ 9.3 and 12.5 ppm, indicating the presence of multiple hydroxyl groups in the structure. The aromatic protons, which are part of an aromatic ring, are seen between δ 6.19 and 7.68 ppm. These signals confirm that the compound has both hydroxyl groups and a benzene ring, consistent with the structure of quercetin. The signals are presented in Table 11.

3.12 ^{13}C NMR Analysis of Sample B40

The ^{13}C NMR spectrum of sample B40 shows a key signal at δ 175.9 ppm, indicating the presence of a carbonyl (C=O) group. Other peaks between δ 93.0 and 164.1 ppm correspond to carbons in an aromatic ring, including those attached to hydroxyl groups. This data confirms that the compound contains both a carbonyl group and a hydroxyl-substituted benzene ring, which is characteristic of quercetin.

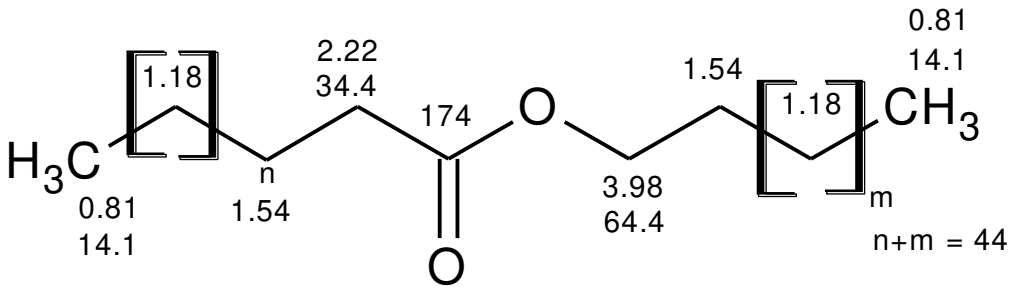

Fig. 4. Chemical structure of sample AZ (Docosanoic acid, nonacosyl ester)

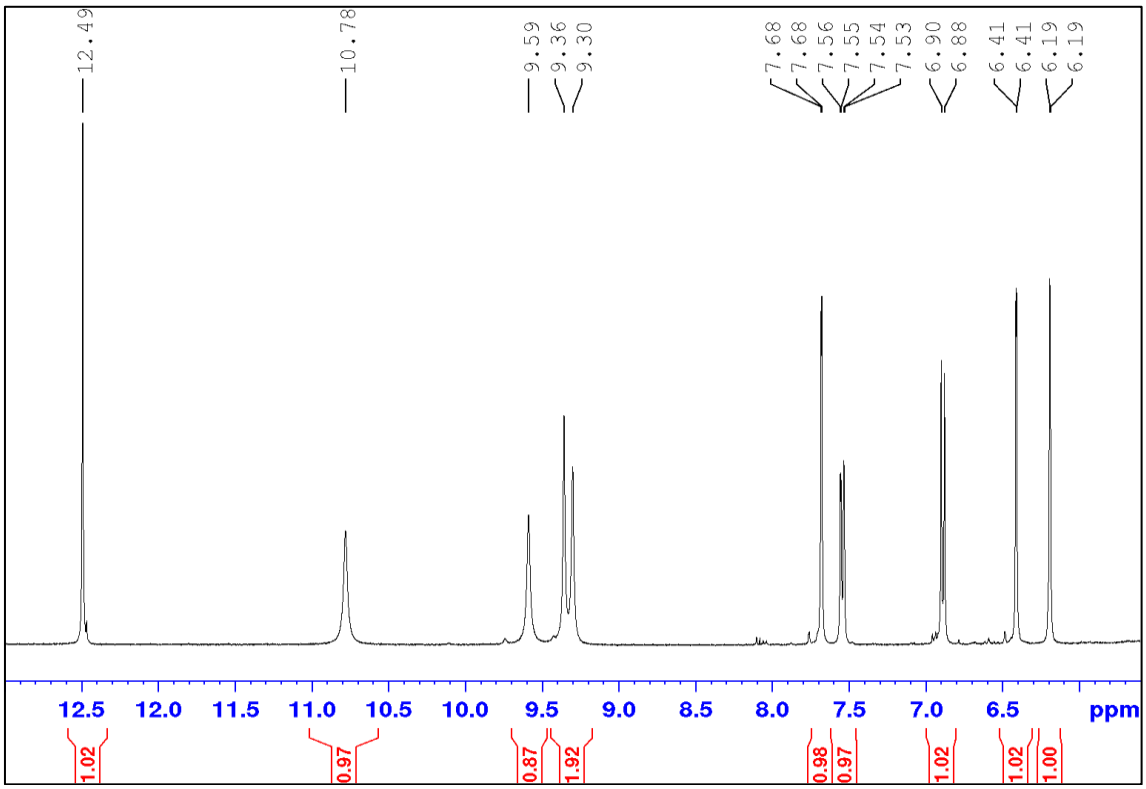

Fig. 5. ^{1}H NMR spectra of B40

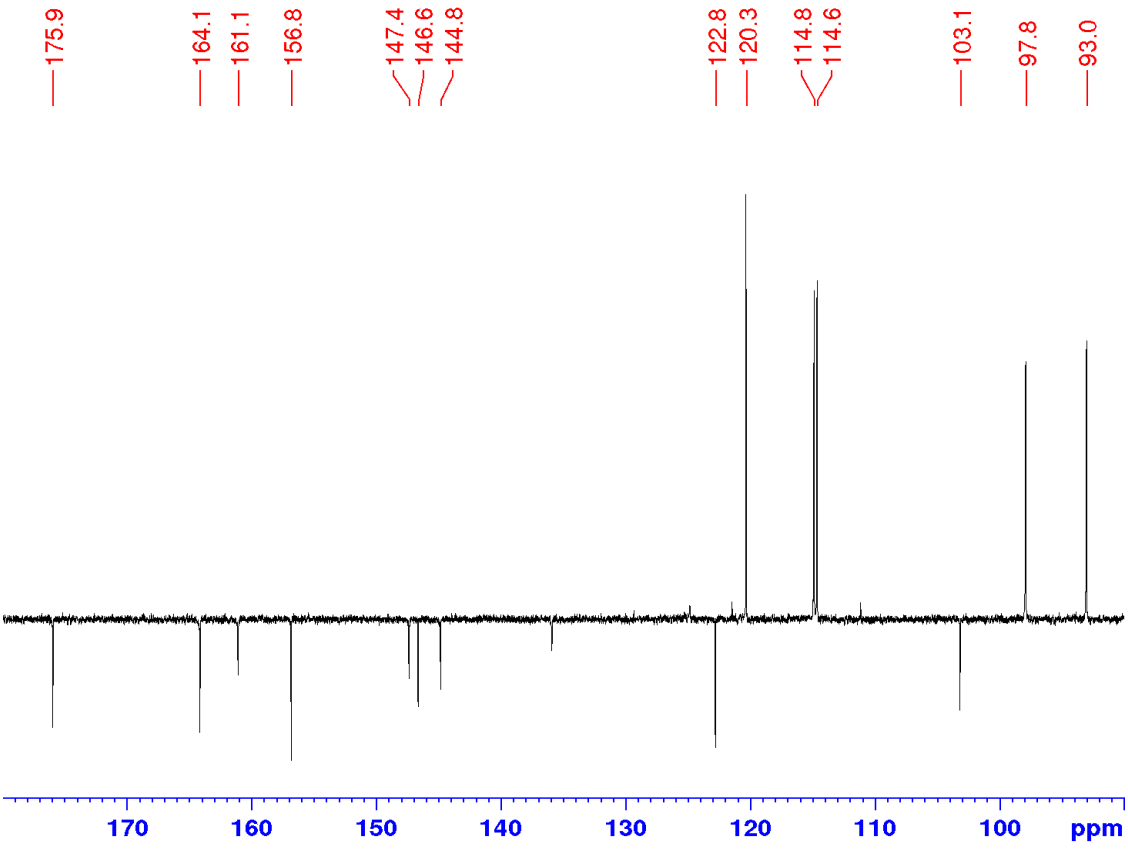

Fig. 6. ^{13}C NMR spectra of B40

Table 11. Data from ^{1}H NMR spectra of sample B40

Peak (δ ppm)	Multiplicity	Number of Protons (Sample B40)	Literature Peaks (Wishart et al., 2008)	Functional Group/Assignment	Significant Peaks for Identification
12.5	s	-OH	12.5 s	Hydroxyl proton (-OH)	Yes, confirms hydroxyl group
10.8	b	-OH	10.5–11.0 b	Hydroxyl proton (-OH)	Yes, confirms hydroxyl group
9.6	b	-OH	9.5–9.7 b	Hydroxyl proton (-OH)	Yes, confirms hydroxyl group
9.4	b	-OH	9.3–9.5 b	Hydroxyl proton (-OH)	Yes, confirms hydroxyl group
9.3	b	-OH	9.2–9.4 b	Hydroxyl proton (-OH)	Yes, confirms hydroxyl group
7.68	d (J = 2 Hz)	1H	7.6–7.7 d	Aromatic proton (C-H)	Yes, confirms aromatic ring
7.54	dd (J = 8.5, 2 Hz)	1H	7.5–7.6 dd	Aromatic proton (C-H)	Yes, confirms aromatic ring
6.89	d (J = 8.5 Hz)	1H	6.8–7.0 d	Aromatic proton (C-H)	Yes, confirms aromatic ring
6.41	d (J = 1.8 Hz)	1H	6.3–6.5 d	Aromatic proton (C-H)	Yes, confirms aromatic ring
6.19	d (J = 1.8 Hz)	1H	6.1–6.2 d	Aromatic proton (C-H)	Yes, confirms aromatic ring

Table 12. Data from the ^{13}C NMR spectra of sample B40

Peak (δ ppm)	Sample B40	Literature Peaks (Wishart et al., 2008)	Functional Group/Assignment	Significant Peaks for Identification
175.9	Present	175–176	Carbonyl group (C=O)	Yes, confirms carbonyl group (C=O)
164.1	Present	163–165	Aromatic C attached to O (C-OH)	Yes, confirms hydroxyl group on ring
161.1	Present	160–162	Aromatic C attached to O (C-OH)	Yes, confirms hydroxyl group on ring
156.8	Present	156–158	Aromatic C attached to O (C-OH)	Yes, confirms hydroxyl group on ring
147.3	Present	146–148	Aromatic C in ring system	No, general aromatic signal
146.6	Present	145–147	Aromatic C in ring system	No, general aromatic signal
144.8	Present	144–146	Aromatic C in ring system	No, general aromatic signal
136	Present	135–137	Aromatic C in ring system	No, general aromatic signal
122.7	Present	122–124	Aromatic C in ring system	No, general aromatic signal
120.3	Present	119–121	Aromatic C in ring system	No, general aromatic signal
114.8	Present	113–115	Aromatic C in ring system	No, general aromatic signal
114.6	Present	113–115	Aromatic C in ring system	No, general aromatic signal
103.1	Present	102–104	Aromatic C in ring system	No, general aromatic signal
97.8	Present	97–99	Aromatic C in ring system	No, general aromatic signal
93	Present	92–94	Aromatic C in ring system	No, general aromatic signal

3.13 FTIR Analysis of Sample B40

The FTIR spectrum data of sample B40 shown in Table 13 reveals important functional groups. A broad O-H stretch at 3243 cm^{-1} confirms the presence of hydroxyl groups, while a sharp C=O stretch at 1662 cm^{-1} indicates a carbonyl group. Additional peaks at 1047 cm^{-1} (C-O stretch) and 721 cm^{-1} (aromatic C-H bend) confirm the presence of alcohol or phenol groups and an aromatic ring. These features align with the structure of quercetin.

Based on the combined analysis of the ^{1}H NMR, ^{13}C NMR, and FTIR spectra, the compound was identified as quercetin. The ^{1}H NMR spectrum reveals signals for multiple hydroxyl (O-H) groups and aromatic protons, confirming the presence of a hydroxyl-substituted benzene ring. The ^{13}C NMR spectrum shows a key carbonyl (C=O) signal at δ 175.9 ppm and additional aromatic carbon signals, further supporting the presence of hydroxyl groups on an aromatic ring. The FTIR data complements these findings, with a broad O-H stretch at 3243 cm^{-1}, a C=O stretch at 1662 cm^{-1}, and a C-O stretch at 1047 cm^{-1}, confirming the hydroxyl and carbonyl groups. Together, these results conclusively identify the compound as quercetin. This was also previously reported in the leaf and seed of *D. tripetala* (Aderogba et al., 2012).

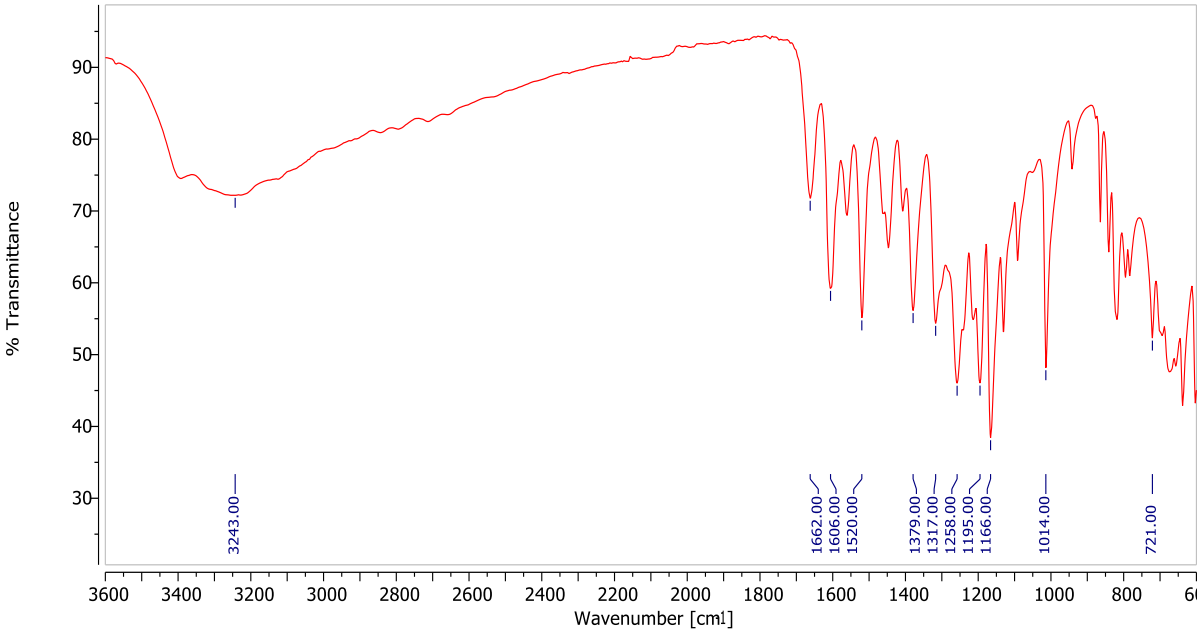

Fig. 7. FTIR spectra of B40

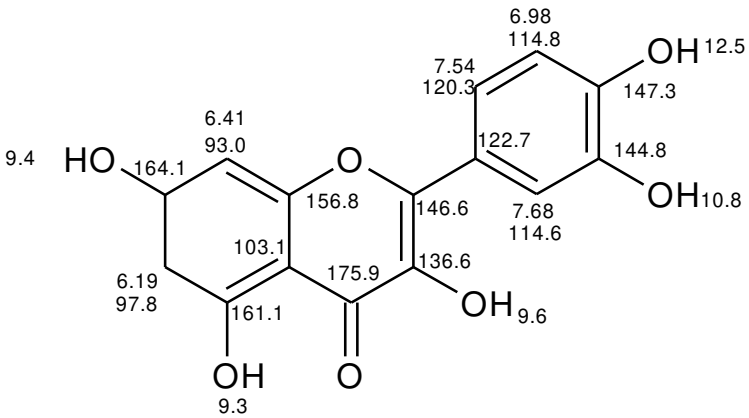

Fig. 8. Chemical structure of sample B40 (Quercetin)

Table 13. FTIR data from the FTIR spectra of sample B40

Peak (cm^{-1})	Sample B40	Literature Peaks (Wishart et al., 2008)	Functional Group/Assignment	Significant Peaks for Identification
3243	Present	3200–3500	O-H stretch (Hydroxyl group)	Yes, confirms hydroxyl group
1731	Present	1660–1690	C=O stretch (Carbonyl group)	Yes, confirms carbonyl group
1457	Present	1440–1460	CH_2 bend	No, typical alkyl bending
1047	Present	1000–1100	C-O stretch (Alcohol or phenol)	Yes, confirms hydroxyl groups
721	Present	700–800	Aromatic C-H bend	Yes, confirms aromatic structure

Table 14. ^{1}H NMR spectra data of sample 0X2

Peak (δ ppm)	Multiplicity	Number of Protons (Sample OX2)	Literature Peaks (Costa et al., 2020)	Functional Group/Assignment	Significant Peaks for Identification
13.18	s	-OH	13.0–13.2 s	Hydroxyl proton (-OH)	Yes, confirms hydroxyl group
10.82	b	-OH	10.8–10.9 b	Hydroxyl proton (-OH)	Yes, confirms hydroxyl group
10.35	b	-OH	10.3–10.4 b	Hydroxyl proton (-OH)	Yes, confirms hydroxyl group
8.03	d (J = 8.8 Hz)	2H	8.0–8.1 d	Aromatic protons (C-H in ring)	Yes, confirms aromatic ring protons
6.9	d (J = 8.8 Hz)	2H	6.9–7.0 d	Aromatic protons (C-H in ring)	Yes, confirms aromatic ring protons
6.79	s	1H	6.7–6.8 s	Aromatic proton (C-H in ring)	Yes, confirms aromatic ring protons
6.28	s	1H	6.2–6.3 s	Aromatic proton (C-H in ring)	Yes, confirms aromatic ring protons
5.01	d	-OH	5.0–5.1 d	Hydroxyl proton (-OH)	Yes, confirms hydroxyl group
4.99	d	-OH	4.9–5.0 d	Hydroxyl proton (-OH)	Yes, confirms hydroxyl group
4.7	d (J = 9.3 Hz)	1H	4.6–4.7 d	Hydroxyl proton (-OH)	Yes, confirms hydroxyl group
4.6	t (J = 5.7 Hz)	-OH	4.5–4.6 t	Hydroxyl proton (-OH)	Yes, confirms hydroxyl group
3.85	t (J = 9.3 Hz)	1H	3.8–3.9 t	Sugar protons (-CH) in glycoside	Yes, confirms sugar unit
3.77	m	1H	3.7–3.8 m	Sugar protons (-CH) in glycoside	Yes, confirms sugar unit
3.54	m	1H	3.5–3.6 m	Sugar protons (-CH) in glycoside	Yes, confirms sugar unit
3.39	m	1H	3.3–3.4 m	Sugar protons (-CH) in glycoside	Yes, confirms sugar unit
3.27	m	1H	3.2–3.3 m	Sugar protons (-CH) in glycoside	Yes, confirms sugar unit
3.24	m	1H	3.2–3.3 m	Sugar protons (-CH) in glycoside	Yes, confirms sugar unit

3.14 ^{1}H NMR Analysis of Sample OX2

^{1}H NMR spectrum of sample OX2 shows signals for multiple hydroxyl (O-H) protons between δ 13.18 and 4.6 ppm, along with aromatic protons at δ 8.03–6.28 ppm, confirming the presence of both hydroxyl groups and an aromatic ring. Additional signals in the 3.85–3.24 ppm range indicate protons from a glycoside sugar unit as shown in shown in Table 14.

3.15 ^{13}C NMR Analysis of Sample OX2

Table 15 shows the data from the ^{13}C NMR spectrum of sample OX2. The ^{13}C NMR spectrum reveals a carbonyl (C=O) peak at δ 182.6 ppm, along with aromatic carbons between δ 163.0 and 98.6 ppm. Several peaks between δ 82.1 and 61.8 ppm correspond to carbons in the glycoside unit, confirming the structure of vitexin. The C=O stretch at 182.6 ppm is slightly high for vitexin.

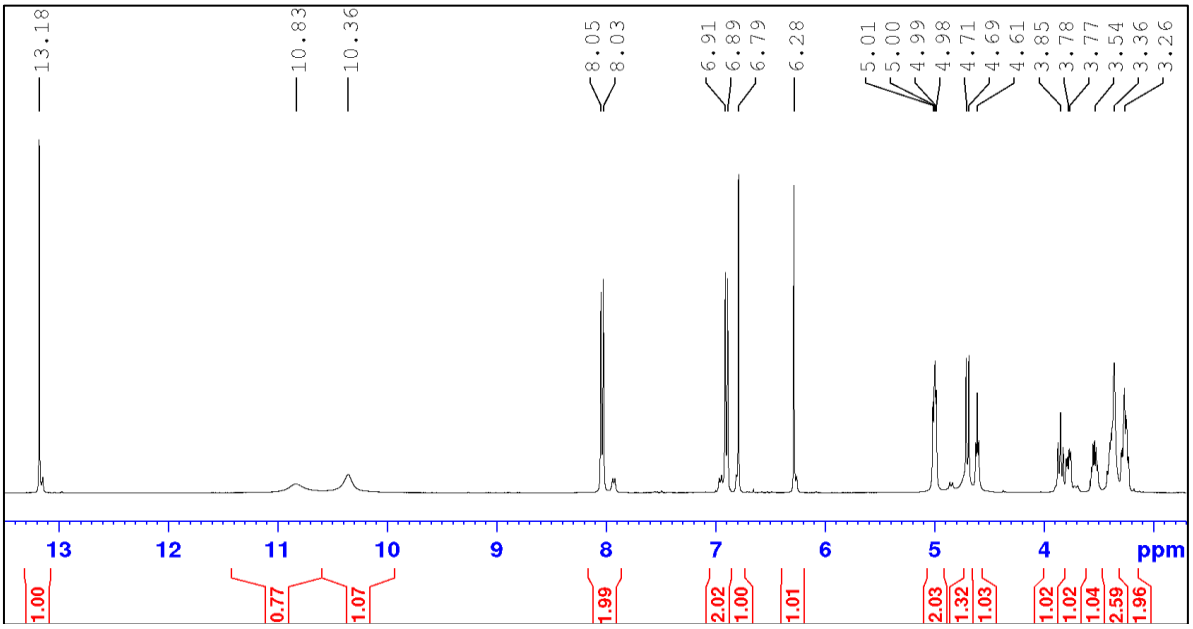

Fig. 9. ^{1}H NMR spectra of OX2

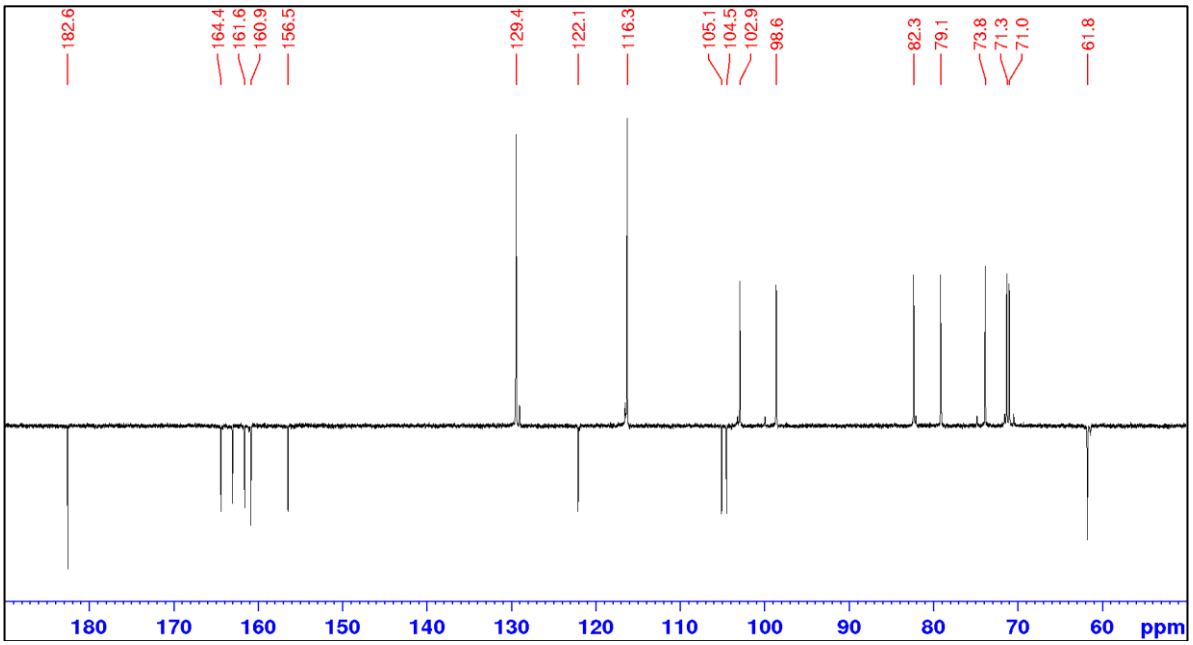

Fig. 10. ^{13}C NMR spectra of OX2

Table 15. Data from the ^{13}C NMR spectra of sample OX2

Peak (δ ppm)	Sample OX2	Literature Peaks (Costa et al., 2020)	Functional Group/Assignment	Significant Peaks for Identification
182.6	Present	180–183	Carbonyl group (C=O)	Yes, confirms carbonyl group
163	Present	162–164	Aromatic carbon attached to O-H	Yes, confirms hydroxyl group
161.6	Present	160–162	Aromatic carbon attached to O-H	Yes, confirms hydroxyl group
160.8	Present	159–161	Aromatic carbon attached to O-H	Yes, confirms hydroxyl group
156.6	Present	155–157	Aromatic carbon	No, general aromatic carbon signal
129.4	Present	128–130	Aromatic carbon	No, general aromatic carbon signal
122.1	Present	121–123	Aromatic carbon	No, general aromatic carbon signal
116.3	Present	115–117	Aromatic carbon	No, general aromatic carbon signal
105.1	Present	104–106	Aromatic carbon	No, general aromatic carbon signal
104.5	Present	104–106	Aromatic carbon	No, general aromatic carbon signal
102.9	Present	102–104	Aromatic carbon	No, general aromatic carbon signal
98.6	Present	97–99	Aromatic carbon	No, general aromatic carbon signal
82.1	Present	81–83	Sugar carbon (glycoside unit)	Yes, confirms glycoside unit
79.1	Present	78–80	Sugar carbon (glycoside unit)	Yes, confirms glycoside unit
73.9	Present	73–75	Sugar carbon (glycoside unit)	Yes, confirms glycoside unit
71.3 – 71.1	Present	71–72	Sugar carbon (glycoside unit)	Yes, confirms glycoside unit
61.8	Present	60–62	Sugar carbon (glycoside unit)	Yes, confirms glycoside unit

Table 16. Data from the FTIR spectrum of sample OX2

Peak (cm^{-1})	Sample OX2	Literature Peaks (Costa et al., 2020)	Functional Group/Assignment	Significant Peaks for Identification
3216	Present	3200–3500	O-H stretch (Hydroxyl group)	Yes, confirms hydroxyl group
1731	Present	1650–1680	C=O stretch (Carbonyl group)	Yes, confirms carbonyl group
1457	Present	1450–1460	CH_2 bend	No, typical alkyl bending
1061	Present	1050–1150	C-O stretch (Alcohol or phenol)	Yes, confirms C-O bond in hydroxyl group
970	Present	960–980	=C-H bend	No, general unsaturation signal
831	Present	820–840	Aromatic C-H bend	Yes, confirms aromatic structure

3.16 FTIR Analysis of Sample OX2

The results of the FTIR data of sample OX2 are displayed in Table 16. The FTIR spectrum displays characteristic peaks, including an O-H stretch at 3216 cm^{-1}, a C=O stretch at 1650 cm^{-1}, and C-O stretches at 1061 cm^{-1}, confirming the presence of hydroxyl groups, a carbonyl group, and aromatic structure in vitexin.

Based on the combined ^{1}H NMR, ^{13}C NMR, and FTIR spectral data, the compound OX2 was identified as vitexin. The ^{1}H NMR spectrum reveals multiple hydroxyl protons and signals corresponding to a glycoside unit and aromatic protons, confirming the structure. The ^{13}C NMR data shows a key carbonyl signal (δ 182.6 ppm) and signals consistent with both aromatic carbons and sugar carbons, indicating the glycoside structure. The FTIR spectrum further supports these findings with characteristic O-H, C=O, and aromatic C-H stretches. This was also previously reported in the leaf of *D. tripetala* (Aderogba et al., 2012).

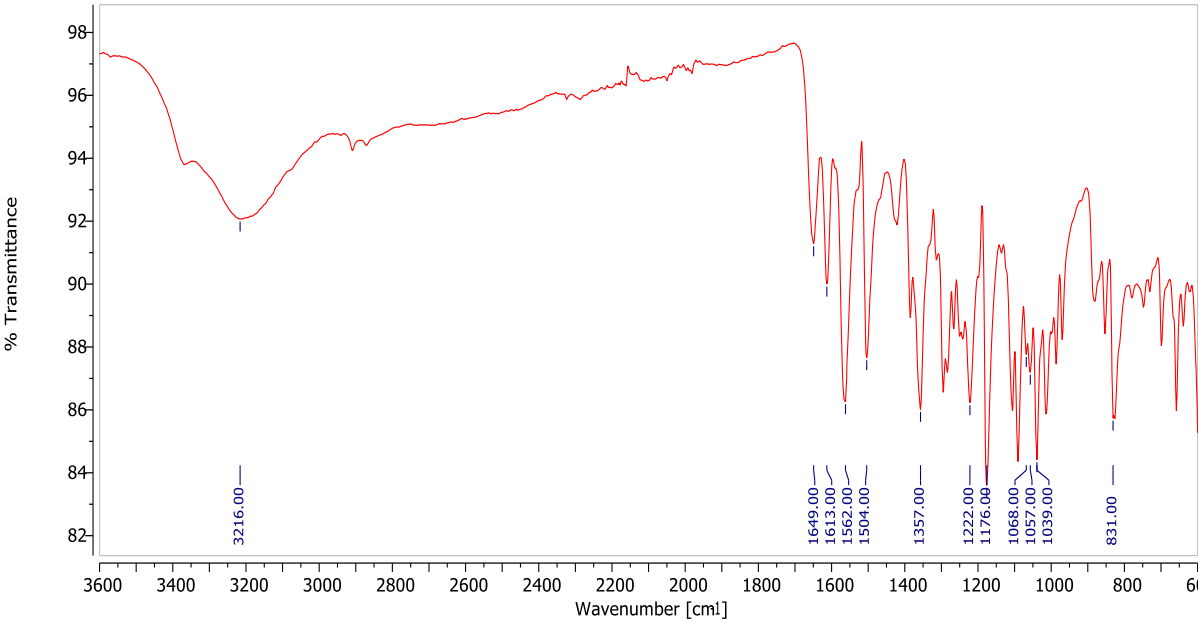

Fig. 11. FTIR spectra of OX2

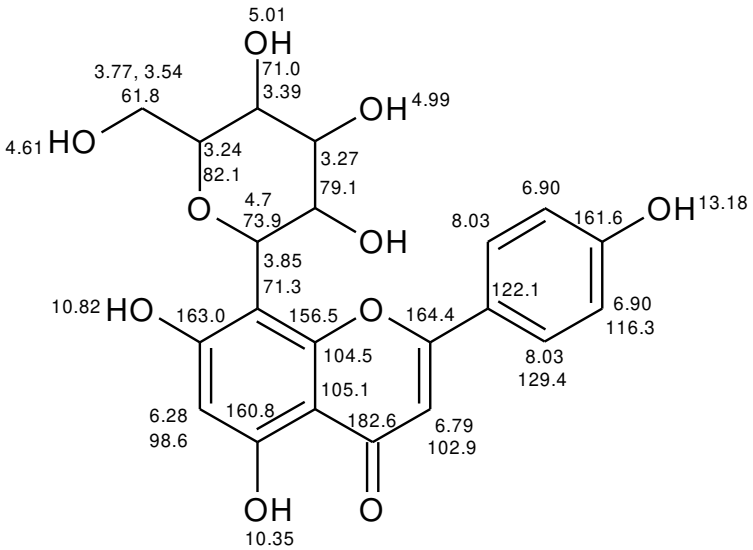

Fig. 12. Chemical structure of sample OX2 (Vitexin)

3.17 Discussion

The root and stem bark of *D. tripetala* and their various fractions demonstrated strong anti-inflammatory and analgesic activities comparable to that of the standard compound Aspirin used in the study. Quercetin is a well-known flavonoid with significant anti-inflammatory, analgesic, and antioxidant properties. It has been shown to inhibit the production of inflammatory cytokines and enzymes, making it a potential therapeutic agent for various inflammatory conditions (Boots et al., 2008). Previous studies have isolated quercetin from *Dennettia tripetala* and demonstrated its potent antioxidant activity (Ugheighele et al., 2022). Vitexin, another flavonoid, has been recognized for its anti-inflammatory and antioxidant effects. It works by inhibiting the production of pro-inflammatory cytokines and reducing oxidative stress (Zhang et al., 2017). The presence of vitexin in *Dennettia tripetala* adds to the plant's medicinal value, supporting its traditional use in treating inflammatory conditions.

Docosanoic acid, a long-chain fatty acid, has been studied for its anti-inflammatory properties. It can modulate inflammatory responses and has been shown to reduce the production of pro-inflammatory cytokines (Kumar et al., 2018). Its presence in *D. tripetala* supports the plant's traditional use in treating inflammatory ailments. *D. tripetala* has been extensively studied for its medicinal properties. Previous research has highlighted its rich phytochemical composition, including alkaloids, tannins, saponins, flavonoids, terpenoids, steroids, and cardiac glycosides (Iseghohi, 2015). These compounds contribute to the plant's broad spectrum of biological activities, such as antioxidant, anti-inflammatory, analgesic, antimicrobial, and cytotoxic properties (Okunlola et al., 2021).

The methanol extract and its fractions of *D. tripetala* have demonstrated significant antioxidant activity, with high concentrations of phenolics and flavonoids contributing to their potency (Dennis-Eboh, et al., 2021). The dichloromethane and ethyl acetate fractions, in particular, have shown potent free radical scavenging activity, supporting their use in managing oxidative stress-related diseases (Ugheighele et al., 2022). These findings align with previous studies and highlight the plant's role in traditional medicine for treating inflammatory, analgesic, and oxidative stress-related conditions.

4. CONCLUSION

This study expands the phytochemical profile of *Dennettia tripetala* by identifying vitexin and docosanoic acid, previously unreported in the plant. It reinforces the plant's anti-inflammatory potential by linking these compounds to its traditional medicinal use. Additionally, it highlights the potent anti-inflammatory activity of its dichloromethane and ethyl acetate fractions, supporting their therapeutic relevance in managing oxidative stress-related diseases.

The research also confirmed that the root and stem bark of *D. tripetala* is rich in bioactive compounds with significant medicinal properties like flavonoids, alkaloids and esters. The research successfully isolated and characterised quercetin, vitexin, rutin, and docosanoic acid, nonacosyl ester which have reported significant anti-inflammatory, analgesic, and antioxidant effects. These findings provide robust scientific support for the traditional medicinal use of *D. tripetala* as an anti-inflammatory agent in African traditional medicine.

DISCLAIMER (ARTIFICIAL INTELLIGENCE)

Author(s) hereby declare that NO generative AI technologies such as Large Language Models (ChatGPT, COPILOT, etc.) and text-to-image generators have been used during the writing or editing of this manuscript.

CONSENT

It is not applicable.

ETHICAL APPROVAL

Permission and approval for animal studies were obtained from the College of Health Sciences Animal Ethics Committee, University of Uyo.

COMPETING INTERESTS

Authors have declared that no competing interests exist.

REFERENCES

Aderogba, M., Akinkunmi, E. O. and Mabusela, W. (2012). Antioxidant and Antimicrobial Activities of Flavonoid Glycosides from Dennettia Tripetala G. Baker Leaf Extract. *Nigerian Journal of Natural Products and Medicine*, 15(1): 49-51.

Adesina, S. K. and Johnny, I. I. (2021). Plants in Herbal Medicine; Their Traditional Uses, Chemistry and Biology. *Book Publishers International, London*. 785pp.

Boots, A. W., Haenen, G. R. and Bast, A. (2008). Health effects of quercetin: From antioxidant to nutraceutical. *European Journal of Pharmacology*, 585(2-3), 325-337.

Dennis-Eboh, U., Achuba, F. I. and George, B. O. (2021). Evaluation of the phytochemical and antioxidant properties of cold, hot water, and wine extracts produced from *Ficus capensis* leaf. *Tropical Journal of Phytochemistry and Pharmaceutical Sciences, 2*(2), 47-54.

Enema, O. J., Umoh, U. F. and Johnny, I. I. (2024): Phytochemical profile and *in vitro* antioxidant evaluation of the root of *Dennettia tripetala* BAK. F. (Annonaceae). *IOSR Journal of Pharmacy (IOSRPHR)*. 14(6): 4-16.

Eseyin, O. A, Akaninyene, D., Thomas, P. S., Attih, E., Essien, E., Johnson, E. C., Zubaid, A. S. M., Ahmad, A., Afzal, S. and Ukeme, A. (2017). Phytochemical analysis and antioxidant activity of the seed of *Telfairia occidentalis* Hook (Cucurbitaceae). *Natural Product Research,* 32(4): 1478-1494.

Hunskaar, S. and Hole, K. (1987). The formalin test in mice: dissociation between inflammatory and non-inflammatory pain. *Pain*, 30, 103-114.

Iseghohi, S. O. (2015). A review of the uses and medicinal properties of *Dennettia tripetala* (Pepperfruit). *National Library of Medicine*, 3(4): 104-111.

Kumar, N., Goel, N. and Pandey, V. N. (2018). Anti-inflammatory and antioxidant properties of docosanoic acid in experimental models. *Journal of Ethnopharmacology*, 214, 1-8.

Lorke, D. (1983). A new approach to tropical acute toxicity testing. *Archives of Toxicology*, 53(1): 275-287.

Mbagwu, H. O. C., Anene, R. A. and Adeyemi O. O. (2007). Analgesic, antipyretic and anti-inflammatory properties of *Mezoneuron benthamianum* Baill Caesalpiniaceae. *Nigerian Quarterly Journal of Hospital Medicine*, 17(3): 35 – 41.

Nwafor, P. A. and Okwuasaba, F. K. (2003). Anti-nociceptive and anti-inflammatory effects of methanolic extract of *Asparagus pubescens* roots in rodents. *Journal of Ethnobiology and Ethnomedicine*. 84: 125 – 129.

Okokon, J. E., Antia, B. S. and Umoh, E. E. (2008). Analgesic and anti-inflammatory activities of *Hippocratea africana*. international journal of pharmacology, 4(17): 51–55.

Okunlola, B. M., Adebiyi, Y. H., Odey, B. O., Alawode, R. A., Lawal, A., Okunlola, B. M., Ibrahim, J. and Berinyuy, E. B. (2021). *Dennettia tripetala* (Pepper Fruit), a review of its ethno-medicinal use, phyto-constituents, and biological properties. *GSC Advanced Research and Reviews*, 6(3), 35-43.

Pahwa, R., Amandeep, G., Pankaj, B. and Jialal, I. (2021). Chronic inflammation. *StatPearls Publishing*. https://www.ncbi.nlm.nih.gov/books/NBK493173/ (Retrieved on August 2021).

Sofowora, A., Ogunbodede, E. and Onayade, A. (2013). The role and place of medicinal plants in the strategies for disease prevention. *African Journal of Traditional, Complementary and Alternative Medicines*, 6(5): 210–229.

Tjolsen, A., Berge, O. G., Hunskaar, S., Rosland, J. H. and Hole, K. (1992). The formalin test: an evaluation of the method. *Pain*, 51: 5 – 17.

Tsai, D. H., Riediker, M., Berchet, A., Paccaud, F., Waeber, G., Vollenweider, P., and Bochud, M. (2019). Effects of short- and long-term exposures to particulate matter on inflammatory marker levels in the general population. *Environmental Science and Pollution Research International*, 26(19): 19697-19704.

Ugheighele, S., Imafidon, K., Choudhary, M., Ahmed, S. and Okoro, E. (2022). Isolation of Quercetin and Avicularin from *Dennettia tripetala* (G. Baker) Seeds, and Evaluation of the Oxidative Stress Management Capacity and Cytotoxic Activities of Its Acetone Extract and Fractions. *Chemistry Africa*. 5(3): 413-415.

Vaz, Z. R., Cechinel, V., Yunes, R. A. and Calixto, JB (1996). Antinociceptive action of 2-(-4bromobenzoyl)-3-methy-4-6-dimethoxybenzofuran, a novel xanthoxyline derivative of chemical and thermal models of nociception in mice. *Journal of Pharmacology and Experimental Therapeutics*, 278: 304 – 312.

Zhang, Y., Liu, Y., Wang, T. and Wang, X. (2017). Vitexin protects against oxidative

stress and apoptosis in H9c2 cardiomyocytes via the PI3K/Akt signaling pathway. *Molecular Medicine Reports*, 16(2), 2053-2060.

Peer-review history:
The peer review history for this paper can be accessed here:
https://pr.sdiarticle5.com/review-history/132064